Scientific Visualization, 2022, volume 14, number 3, pages 92 - 106, DOI: 10.26583/sv.14.3.07

Single Image DnCNN Visibility Improvement (SImDnCNNVI)

Sangita Roy[1]

ECE Department Narula Institute of Technology, Kolkata, India

[1] ORCID: 0000-0002-8898-0183, roysangita@gmail.com

Abstract

The presence of fog, haze, or atmospheric particles reduces visibility which is an under-constrained challenging classical problem due to ambiguous scene radiance and transmission. Consequently, digital images captured under such conditions suffer from poor recognition. In this work, a fast single image physics based inversion scattering model is adopted to overcome these limitations. Denoising convolutional neural networks (DnCNNs) model is well suited for blind Gaussian denoising in a learning framework at hidden layers. With the DnCNN blind denoised depth map, high-quality transmission is estimated and finally by inverting scattering image formation model, a clear image is obtained along with tuned haziness factor. The proposed algorithm performs well compared to sixteen state-of-the-art methods qualitatively and quantitatively on Ground Truth (GT) O-Haze dataset. Output images are appealing, halo free, edge preserved, colour balanced, clear.

Keywords: Image recovery model, Quality Assessment, DnCNN, Residual Learning, Batch Normalization, Dehazing, extinction coefficient.

1. Introduction

Image with fine details is the key for image analysis, and extraction. Haze, fog, and suspended particles in the atmosphere cause obstacles in image visibility due to the scattering of light in the media by those suspended particles [1, 2].Visibility is one of the research sought-after topics during the last decade. Thousands of research papers are found to address the problem [3]. Several techniques have been proposed till now. As the problem is ill-posed and prediction-based, no single method can validate the problem. Dehazing, defogging, and deraining techniques are classified into three broad categories, (i) Image enhancement based, (ii) Image Fusion based, and (iii) Image Restoration based [3]. The image Enhancement method takes care of the contrast and visual effect of the image without taking care of image degradation. The image fusion-based method highlights the maximization of information from multiple sources of images. The image restoration-based method finds the optical-based physics model to invert the degraded image and compensate for the distortion by some statistical prior. Among the three categories, image restoration methods address the dehaze problem precisely until now. The image formation optical model was first proposed by H. Koschmieder [10] and improved by MacCartney [11].

In [9] pioneering work of Oakley et al. for the first time proposed an image formation scattering model to fix the problem of visibility improvement. They have solved the inverse model with scattered and attenuated relative pixel flux estimation. Finally, this estimated attenuated map was subtracted from the hazy image to produce a clear image. A temporal filter is presented to solve the problem.

Tan [4] in 2008: The work of Oakley [9] improved contrast. Further in [4], the transformation of one gray image into a color image was performed under the two preceding conditions, i. the contrast in the clear image should be higher than that of the hazed image, ii. Attenuation of field spots is a continuous function of distance and gradually becomes smooth.

Fattal [5] in 2008: In [5], the novel prior estimation described no correlation between object surface shading and the transmission map. Independent component analysis (ICA) and a

Markov random field (MRF) model applied to estimate the surface albedo. Thus, it quantified the medium transmission of the scene and recovered the clear image from the hazy image.

J Kopf et. al. [29] in 2008: established an intrigued system of browsing, enhancing, and manipulating outdoor photographs in association with already existing GIS digital terrain and urban models. Thus, the generated image is of high quality, and clear, but requires expensive infrastructure and offline processing is used.

He et al. 's [6]: Dark channel prior (DCP) is undoubtedly a milestone work of the dehazing problem. It triumphs over the drawbacks of the above-mentioned algorithms. A clear image has a minimum intensity in a patch out of a colour channel. This principle is the soul of the model, which was then applied to atmospheric scattering models and developed marvellous results. It combines with soft matting for master stroking the restoring image, which is responsible for high computational complexity.

Tarel et al. 's [7]: developed a fast contrast-based enhancement to remove haze with linear complexity. The atmospheric veil function was considered locally changeable slowly, thus the extinction coefficient of the medium was estimated. The transmission coefficient of the medium was estimated by pretreatment and median filtering. White balancing was applied to smooth the heterogeneous medium.

Berman et al. 's [8]: It is non-local prior with nonuniform degradation. The proposed method introduced colours of the haze-free image to be clustered firmly and spread over the entire RGB image depending on their different transmission coefficients. Whereas a hazy image forms a strong line of colours that was earlier clustered, called the haze line. It recovers distance maps and haze-free images reproduce from the haze line. The algorithm is linear, faster, deterministic, no training is required.

K Zhang [30]: In [30] 2017 a novel idea was introduced with the DnCNN model that utilized batch normalization and residual connection for blind Gaussian denoising. DnCNN is a Trainable Non-linear Reaction-Diffusion (TNRD) Model for fast and effective image restoration.

Y Chen [31] in 2015: TNRD – In [31] described TNRD (Trainable Nonlinear Reaction-Diffusion) based image restoration with highly parameterized linear filter followed by highly parameterized influence functions through training of a loss-based approach. It is equally applicable for image Gaussian denoising, super-resolution, and deblocking.

Kim et. Al. [35]: Contrast of hazy images enhanced by minimum information loss as cost function compensation. Static image and video are processed in real time. Flickering artifacts in video and ringing artifacts in still images are removed [35].

Kolar: Non-homogeneous illumination is corrected with optimization of parameters of B-spline shading model to Shannon's entropy on Parzen windowing. Gradient-based optimization algorithms efficiently use the derivatives of entropy. The work investigates extensively large retinal images to improve inhomogeneity in illumination [36].

PSAC (Photoshop Auto Contrast algorithm): is widely used in photoshop images for contrast improvement [37].

Tang studied in depth different haze-relevant features, especially DCP, in a learning framework to extract the best dehazing feature combination. The synthetic hazy dataset, as a training set, was found effective for dehazing real-world data [38].

Xiao [39]: Real-time single image retinex based color preservation method for defogging is presented. The method restores clear images from foggy images with real colour and a real-time basis.

Contribution: Efficient and effective results found in [12-15, 32]. Blind gaussian Denoiser (DnCNN) improves depth map quality effectively. Thus, refined transmission maps were extracted. Finally, good quality reconstruction was achieved through the linear optics model. Both DnCNN and optics models are linear.

Fig. 1. Example of a) Sample hazy image (b) Dehazed image

The rest of this paper is arranged as follows. The image formation model has been discussed with mathematical details and related works in section 2. In section 3, the experiment with qualitative and quantitative analysis is examined in detail. Section 4 provides a summary of the work and recommends future research directions and shortcomings.

2. Proposed Approach with Related work

In prior knowledge-based dehazing, original scene radiance is recovered through the degradation model, and Physics-based optical scattering model shown respectively in figure 2 and figure 3.

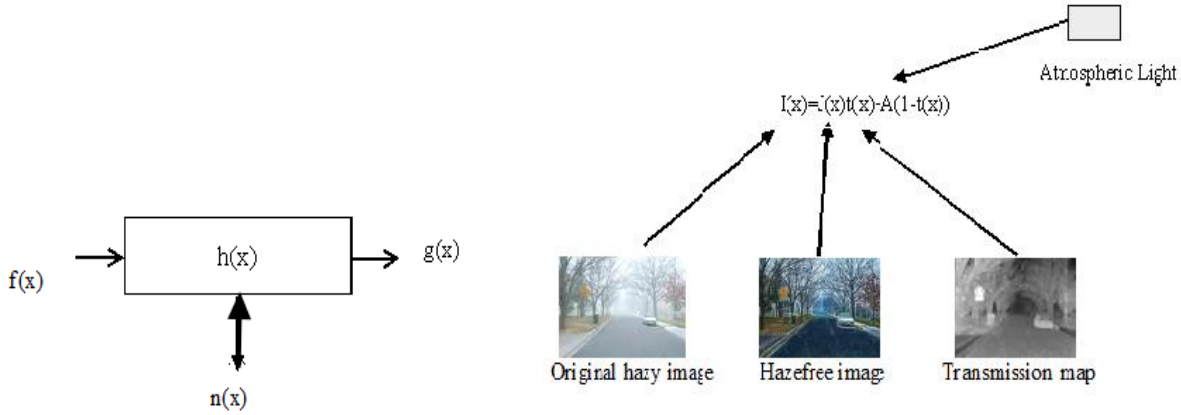

Figure 2. a. Image Degradation Model (Left), b. Image Formation Optical Model

$$g(x) = f(x) * h(x) + n(x) \tag{1}$$

2.1 Physical based optical scattering model:

This model relies on Mie scattering [10,11]. In [9] experimented with this model for the first time to improve image quality under poor visibility conditions. Since then, this problem has been a research hotspot. Image captured by the camera is divided into two parts, one is direct attenuation of light from the original scene to the camera or observer, and the other is a scattering of atmosphere light ending up at the camera. Thus, the final image at the observation point is blurry, low contrast, poor visibility, and noisy. This mechanism is expressed in figure 2b and represented by equation (2)

$$I(x) = J(x)t(x) + A\big(1 - t(x)\big) \quad (2)$$

where I(x) is a degraded image, J(x) represents original scene radiance, t(x) is transmission map and A is Atmospheric light. Three variables, J(x), t(x), and A are unknown. Single image dehazing is an under-constrained problem. Efficient estimation of t(x) and A is the key to effective haze removal. Thus, optimum estimation of t(x), and A are the key to restore J(x). t(x) is estimated from depth estimation, multiple images, or from some prior with a single image. But estimation of the unknown parameters leads to the overall problem of the ill-posed inverse problem or constrain / intractable optimization problem. J(x)t(x) term is known as direct attenuation as original scene radiance reduces exponentially with distance. A(1-t(x)) is called an atmospheric veil, airtight, atmospheric scattering light which causes shifts of colour, and degradation of the scene.

2.2 DnCNN Architecture and noise estimation

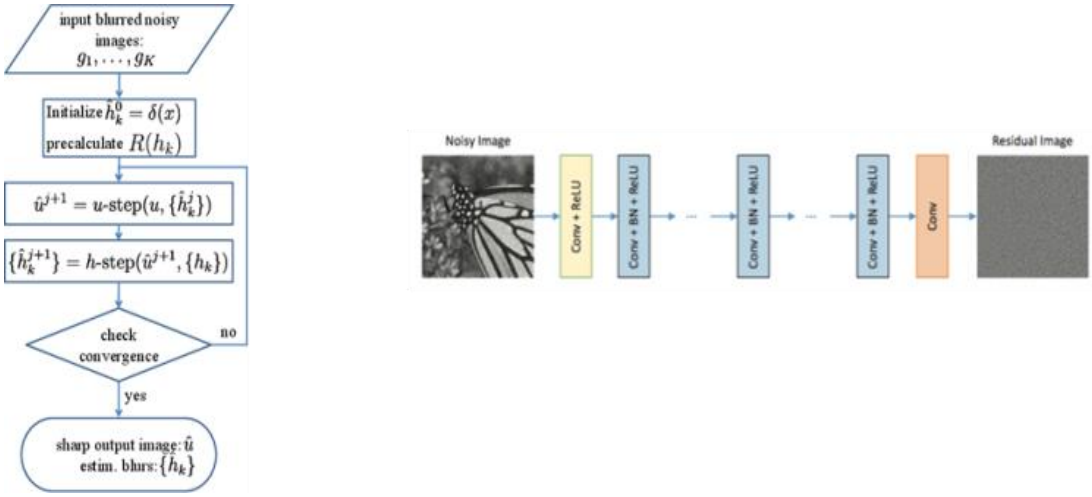

Figure 3 a. Flow Chart [DnCNN] (Left); b. DnCNN network Architecture [DnCNN] (Right)

DnCNN is a feedforward very deep Convolution Neural Network for denoising under discriminative learning of research hot spots. This architecture incorporates a learning algorithm with regularisation. Residual learning and batch normalization are incorporated to speed up the training process towards denoising performance boost up. This model in figure 4 removes s efficiently blind Gaussian noise. Thus, the model can perform cleaning the noise in the hidden layers. These features attract several applications like jpeg image artifact removal, single image super-resolution, image deblocking, GPU computing [DnCNN]. Any deep CNN involves two steps:(i) network architecture design (hereby VGG) and (ii) model learning from training data (residual learning speed up and better-denoised performance with batch normalization) [30].

a. *Network Depth*

Convolution kernel of 3x3 size without any pooling layers. The receptive field of d depth is (2d+1) (2d+1). Increased size of the receptive field tends to grasp a larger image area so that trade-off between performance and efficiency is an important issue in designing DnCNN with proper depth d. Receptive field size relates to the patch size of the demonizing model used. Highly noised zones require larger patch sizes for effective reconstruction. DnCNN uses σ =25 as noise level,

b. Network Architecture

Input to DnCNN is noisy. y=x+v. According to discriminative learning like MLP (Multilayer Perceptrons), CSF (a cascade of shrinkage fields), mapping function $\mathcal{F}(y)=x$ estimates clean image. In the DnCNN model, $\mathcal{R}(y)\approx v$, residual mapping, is extracted from residual learning. Thus, $x=y-\mathcal{R}(y)$. Now, the average mean square error between residual images and estimation from noisy input is

$$l(\Theta) = \frac{1}{2}\sum_{i=1}^{N} \|Ry_i, \Theta - (y_i - x_i)\|_F^2 \quad (3)$$

This is also considered as a loss function to learn the trainable parameter Θ. $\{(x_i, y_i)\}^{Ni}_{=1}$ signifies N noisy-clean image pairs. Figure 3 shows a proposed model to learn residual images.

Deep Architecture

There are three types of architecture.: i. conv+ReLU, first layers 64 filters with 3x3xc size for 64 features maps along with ReLU unit (ReLU, max (0,.)) for nonlinearity, (c-number of image channels). ii. Conv+batch normalization_ReLU- Batch normalization is performed in-between convolution and ReLU. 64 filters with 3x3x64 size are for 2~(d-1) depth hidden layers. iii. Convolution is for the last layers for reconstructed output.

Removal of Boundary Artifacts

To maintain the size of the output image as that of input, zero paddings are maintained before convolving. This way boundary artifacts are removed.

c. Unification of Residual Learning and Batch Normalization for Image Denoising:

The model in figure 1 is equally efficient to produce x from $\boldsymbol{\mathcal{F}}$(y) or $\boldsymbol{\mathcal{R}}$(y) to predict noise v. The benefit of ReLU and Batch Normalization is used not only to speed up performance but also to estimate F(y) as close as clean image X with the estimation of residual image v. Residual learning is integrated with batch normalization to speed up and to cope up the performance due to internal covariate shift during parameter training. Finally, Bath normalization boosts denoising performance the best.

d. Association with TNRD

The DnCNN model proposed is a one-stage TNRD (Trainable Nonlinear Reaction-Diffusion) model. Initially, TNRD was developed to address the problem below

$$\Psi_y - x + \lambda \sum_{k=1}^{K} \sum_{p=1}^{P} p_k f_k * x_p \quad (4)$$

It is defined as a huge set of noisy-clean image pairs, N -the number of image size, ƛ -the regularisation parameter. f_k * x represents the convolution of image x with kth kernel f_k. $p_{k(..)}$ indicates the tunable kth penalty function in the parameter TNRD model. In Gaussian denoising $\psi Z = \frac{1}{2}\|Z\|^2$**.** The first stage diffusion iteration is represented as one gradient descent inference step starting at point y

$$X_1 = y - \alpha\lambda \sum_{k=1}^{K} \bar{f_k} * \phi_k f_k * y - \alpha \frac{\delta \psi z}{\delta z}|_{z=0} \quad (5)$$

$\bar{f_k}$ is obtained by 180º phase shift of filter f_k , also known as adjoint of filter f_k. α is the step size. $\rho'(.) = \phi_k(.)$ and $\frac{\delta \psi z}{\delta z}|_{z=0}$. Thus, equation 3 turns to the equation

$$V_1 = Y - X_1 = \alpha\lambda \sum_{k=1}^{K} \bar{f_k} * \phi_k f_k * y \quad (6)$$

v_1 is the estimated residual of x w.r.t y. The effect of influence function ϕ_k (.) is considered as pointwise nonlinearity applied on convolutional feature maps. Equation 4 represents 2-layers feed-forward CNN. DnCNN of figure 3 is regarded as generalized TNRD with i. Replacement of the influence function with ReLU simplifies CNN training, ii. The capacity of image modeling increases as the depth of CNN increases, iii. Batch normalization boosts CNN performance. Most of the DnCNN parameters represent image priors. Though the DnCNN model is basically for Gaussian noise, equally applicable for any type of noise. v_1 can be obtained from equation (3) if

$$\frac{\delta \psi(z)}{\delta z}|_{z=0} = 0 \quad (7)$$

Equation (5) is applicable for any kind of noise. Thus, the DnCNN model is used efficiently to remove SSIR, JPEG artifacts and to clean hidden layers.

e. Tending to General Image Denoising:

The Gaussian denoising model is best suitable for a fixed noise level. Thus, before cleaning, the noise level is estimated and scaled down to a particular level and then applied to the model for efficient results. Training images are with AWGN from a wide range of noise levels, down-sampled images with multiple upscaling factors, and JPEG images with different quality factors. This method is performed excellently not only on blind gaussian image denoising but also on image deblocking, SISR (Single Image Super-Resolution), and blind image denoising.

2.3 DnCNN network in the Proposed Model

Refined transmission is achieved from turbid transmission via an approximate depth map (minimum intensity channel in the proposed model). The finer depth map is denoised with blind gaussian DnCNN in a learned framework through hidden layers. Equation (2) is the optical physics-based image degradation model [1,2]. I(x), J(x), t(x), A, and d are degraded images, original image, transmission, atmospheric light, and distance respectively. β is the extinction coefficient of the atmosphere and is represented as

$$t = e^{-\beta d} \tag{8}$$

J(x)t(x) term is responsible for direct attenuation and the A(1-t(x)) term represents airlight. These two terms are the reason behind the hazy model. Direct attenuation deteriorates the brightness of pixels as it traces away from the source. Whereas airtight term causes the pixel intensity white or grey as transmission decreases. It is clear from equation (2) that the airtight term is additive. Therefore, as transmission decreases, brightness increases while colour fades or saturates less. During the transmission from the original scene point to the acquisition point, each pixel gets corrupted with additive as well as multiplicative noise. This noise shifts colour, contrast, brightness, and sharpness of the pixel, and makes the resulting image whitish and almost invisible. Mathematically, as d tends to infinity, t(x) tends to zero. Consequently, I(x) tends to A. This is the reason that far objects are whitish and gradually vanish [27]. Single image haze removal becomes difficult to solve. A minimum of three RGB - channels is chosen as a depth map [12,13] and refinement is done using DnCNN on depth map to get noiseless output which will produce clear transmission estimation. This is shown in equations(9), (10) and (11).

$$I_{cmin} = (I^c(x)) \tag{9}$$

I^c and Icmin indicate each RGB or multi-channel of an image and at least three or more channels respectively. The minimum intensity channel I_{cmin} can now be considered as a raw depth map to recover haze-free image and easily be made noise-free or smoothened with the DnCNN technique shown by equation (9).

$$I_{cminDnCNN} = DnCNNI_{cmin} \tag{10}$$

Equation (10) shows a noise-free minimum intensity channel or refined depth map. This channel is normalized. Compliment of this equation will produce a maximum intensity channel with DnCNN to reconstruct prominent image structure and reduced computational complexity and easy to implement as transmission estimation t(x). With DnCNN, good quality haze-free images will be generated without compromising the important structure of the original image. To generate a depth map by minimum patch estimation is more accurate, but computationally expensive [7]. The final refined transmission is represented by equation (11).

$$t_{new}x = 1 - kI_{cminDnCNN} \tag{11}$$

t_{new},k are refined transmission and a proportionality constant for aerial perspective respectively[33,34]. The value of k is between 0 to 1, clear visibility to no visibility. The concept of k, haziness factor, discussed in detail [7,12-15,32,43] and has been chosen dynamically for flexible, visually pleasing images. Atmospheric light is estimated as the average of the top 1% pixel intensity of each channel. Estimated transmission and atmospheric light help to revive

original scene radiance J(x) from equation (2) and can be rewritten as in Eq. (12). This method is shown in figure 4. The process is shown pictorially in Figures 5, 6 in detail.

$$Jx = \frac{Ix - A}{max(tx, t_0)} + A \tag{12}$$

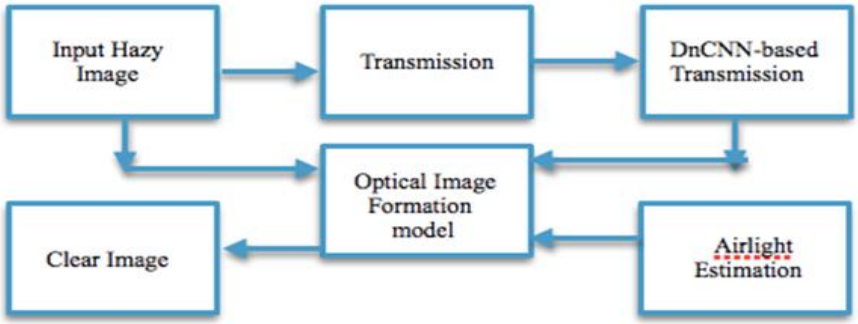

Fig 4 Block Diagram of SImDnCNNVI Model

Figure 5. Analysis of the SImDnCNNVI model, Input, Depth map, transmission, output, improved depth map, improved transmission map, Improved output, a depth map of the final output, transmission map of the final output (L-R).

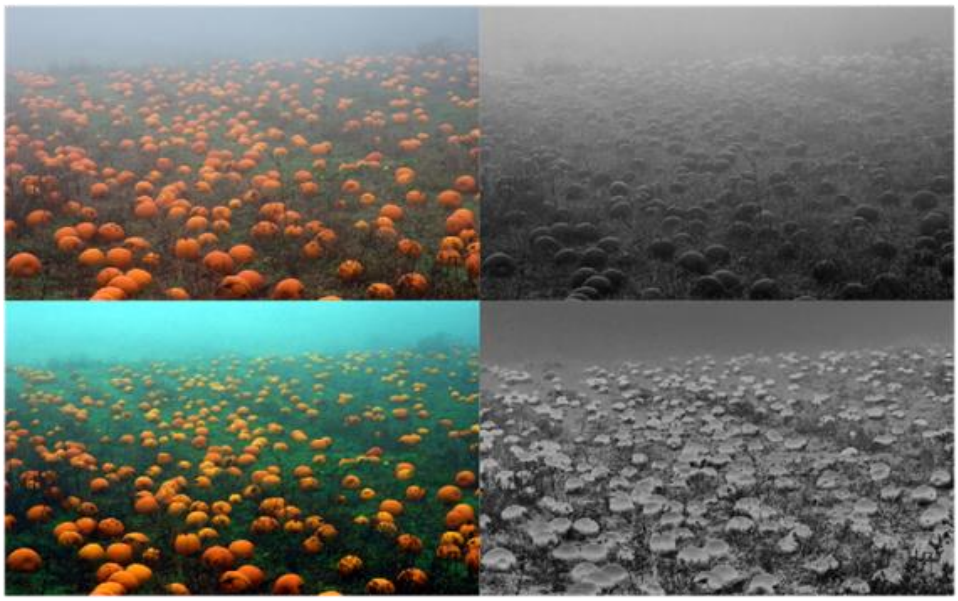

Figure 6. Top L-Input, R-Depth map; Bottom L- Output, R-Depth map

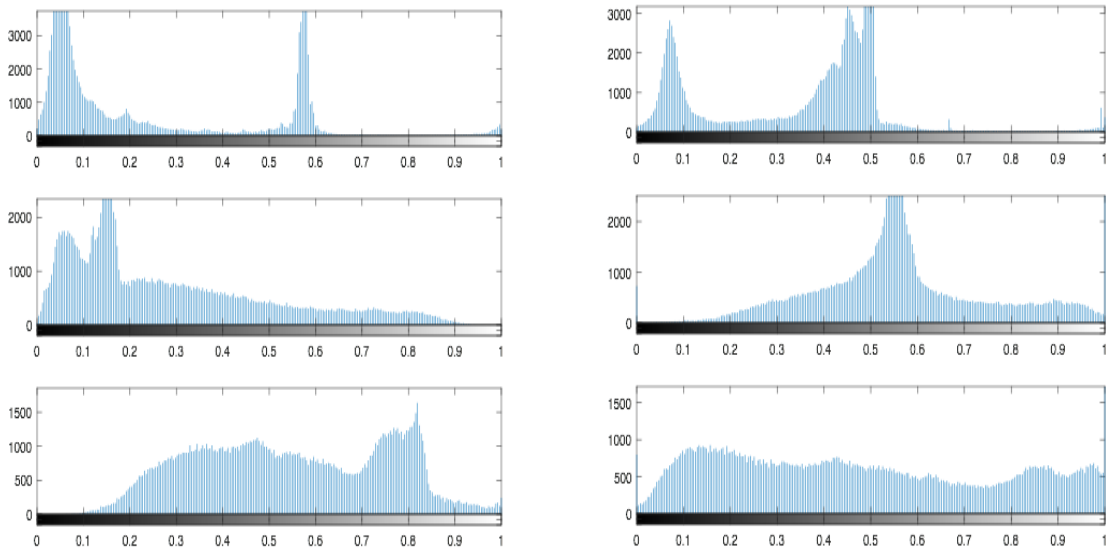

Figure7 L-R; Top Hue, middle-saturation, Bottom-Value: of Hazy Input; Top Hue, middle-saturation, Bottom-Value of Improved Output

In figure 7, the hue, saturation, and value channel of input (left) and output(right) are shown. The saturation and value channel histogram of the output image is more distributed than its hazed version. That indicates the quality of the image gets improved while the hue channel is almost the same. Thus, colour attenuation is prevented, while colours are tending to saturate, and brightness increases with contrast. As a whole, direct attenuation terms are less affected after rectification while airtight term decreases.

3. Experiments

To verify the usefulness of the SImVIDnCNN model, we performed extensive experiments on both synthetic and natural hazy image datasets [Frida, He, O-Haze] and compared them with seven state-of-the-art methods. The experiment is run on Matlab18a with the SImVIDnCNN model. For synthetic datasets, we evaluate our results quantitatively and qualitatively. For the natural hazy image dataset, we provide qualitative results to illustrate our superior performance in generating perceptually pleasing and haze-free images.

3.1 Subjective Evaluation of Various Methods on

Four images are selected from the Frida data set for comparison experiment. These images are natural and have large sky areas which create a halo effect and blocking artifacts at the time of dehazing. Figure 8 contains four hazy images and their depth map, transmission estimation, and haze-free images. Output images are halo effect-free, nature colour preserved, visibly clear. Figure 9 presents one sample image which is experimented for comparative analysis with five state-of-the-art methods. It is evident from the fig 9 that the proposed method gives more visibility and visually pleasing image. Especially, the sky region gives no reflection that is a very common problem of dehazing methods. Now, synthetic Frida Dataset has also experimented with four images. Figure 10 shows those four synthetic low visible images in the top row and SImDnCNNVI Dehazed output in the bottom row. This method is equally efficient in removing haze from synthetic hazy images like natural images. Trees, buildings are invisible in the synthetic hazy images, whereas its dehazed results are visibly clear. Ten images from the O-Haze dataset are experimented with proposed algorithm and compared to GT and seven benchmark algorithms. The results of proposed work are really satisfactory shown in table V.

Figure 8 Four images a. Hazy, b. Depth Information, c. Transmission Estimation, and d. Dehazed Output

Figure 9 y16_photo.png with different state-of-the-art techniques(Fattal, He, Kopf, Tan, Tarel) and proposed work

3.2 Quantitative Assessment

Subjective tests are biased [41]; quantitative assessments are before investigated for experiments. PSNR, SSIM, Entropy, compression ratio are few criteria for effectiveness. In Table- I, SSIM, PSNR, Entropy (hazy, and haze-free) performance experiment with the proposed method and four images of figure 8. Experimental results show that the SImDnCNNVI model is efficient and effective. SSIM is appreciable with an average of 0.7232, PSNRs are also high (average12.6150), the entropy of haze-free images is higher than hazy images. In figure 9, Objective Analysis one sample image with the state-of-the-artwork of Fatal, He, Kopf, Tan, Tarel, and the proposed work is compared. As reflected from table II, proposed approach outperforms in compression ratio, entropy parameters. Other parameter's values are not bad. Therefore, the testing report finds good results.

Table I Objective Assessment of proposed method with SSIM, PSNR, and Entropy of figure 8

Parameter	Figure 1	Figure 2	Figure 3	Figure 4	Average
SSIM/ PSNR	0.8108/ 15.558	0.7549 / 13.0963	0.6413/ 9.046	0.6858/ 12.7598	0.7232/ 12.6150
Entropy(Hazy) / Entropy(Dehazed)	7.6291/ 7.9181	7.5748/ 7.6003	7.2431/ 7.4524	7.6132/ 7.6998	7.51505/ 7.66765

Table II Objective Analysis one sample image with the state-of-the-artwork of He, Tan, Tarel, Kopeaf, Fattal, and proposed work in figure 9

Parameter	Fatal	He	Kopf	Tan	Tarel	Our
PSNR/ SSIM	18.2041/ 0.77348	19.6198/ 0.9355	13.5678/ 0.7932	20.8609/ 0.9477	12.4032/ 0.989	18.5097/ 0.817
CR/ Entropy	0.9996/ 7.0655	0.9916/ 7.0667	0.9944/ 7.7048	0.9842/ 7.7915	0.9847/ 7.6291	0.9998/ 7.7999

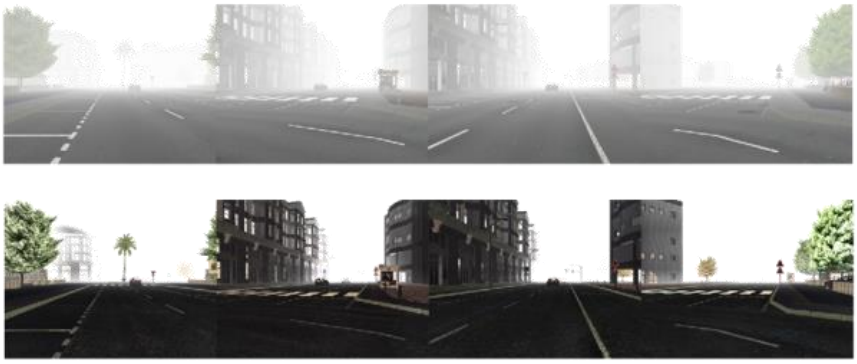

Figure 10 Synthetic Image from Frida2 Dataset a. Hazy Image, b. Dehazed Image

Figure11. More Visual Comparative Analysis

Figure 11 shows an additional visual comparison of different techniques with proposed work. Figure 11 shows that in the proposed method, visibility is greater with small details. Its corresponding objective analysis in table III finds that proposed results are showing good performance over the others. But as the DnCNN is already trained in MATLAB 2018a, running of our program takes very little time whereas all other mentioned methods are offline with high computational complexity. As already explained, the DnCNN model deblocks artifacts and reduces blind noise, thus reconstructed output produces clear images through hidden layers.

Table: III Objective evaluation of Figure 11

Dataset	Parameter	He[6]	Kim[35]	Kolar[36]	Meng[3]	PSAC[37]	Tang[38]	Tarel[7]	Xiao[39]	Ours
IVZ	PSNR/ SSIM	8.3683/ 0.4742	11.3911/ 0.6242	16.8533/ 0.7613	8.3556/ 0.3220	14.0170/ 0.7642	8.2530/ 0.3408	19.4574/ 0.8022	14.9015/ 0.6589	10.3267 / 0.4310
	BRISQE/ NIQE	13.9234/ 3.9057	27.5536/ 4.0779	16.1231/ 3.4152	14.8344/ 3.9095	15.8330 / 3.3367	12.2248/ 4.0374	23.9818/ 3.6162	28.3196/ 3.7914	22.1891/ 6.0818

3.3 More Dehazing with SImDnCNNVI

Images with different degraded forms like underwater, rain, close objects, nighttime, etc were studied, and remarkable results were obtained. This is shown in figure 12 from the frida2 dataset. Therefore, it can be concluded that the proposed approach is equally applicable for any kind of degraded images as well.

Figure 12. Application on nine extreme degraded images of frida2 dataset a. an Input (Top Row), b. It's SImDnCNNVI Dehazing output (Bottom)

Table V:
O-Haze Dataset 10 images:

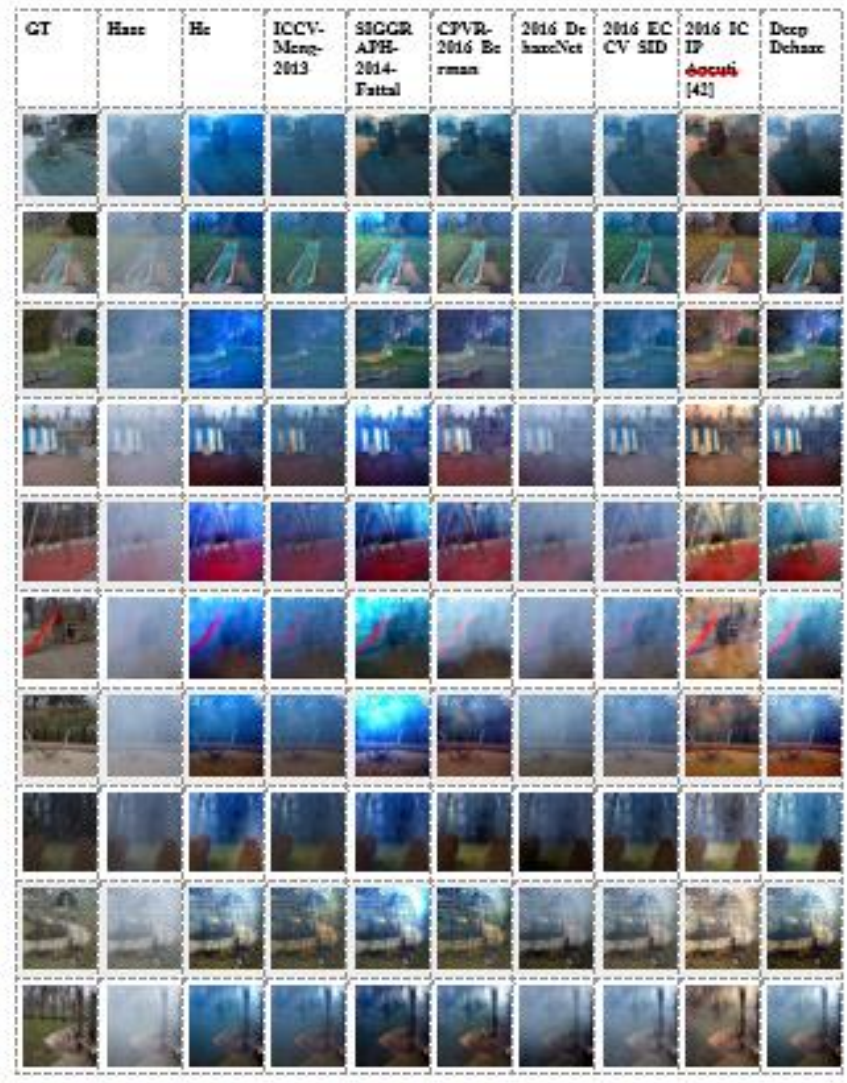

In table V, ten images from the GT O-Haze dataset [42] with seven benchmark algorithms results have been presented and compared with ours. Surprisingly, our results visually outperform almost all others' results. [42] is performing better than ours in some images.

3.4 Run Time

Run time is a factor that evaluates the effectiveness of an algorithm both in time and space. Moreover, the computational power with GPU plays a significant role in the effectiveness of an algorithm. As we are performing our work on Processor INTEL Core i3,3110M CPU@2.40GHz, 64-bit operating system, with MATLAB2018a. Thus, our algorithm is efficient and has low complexity compared to state-of-the-art techniques [He, Fattal, Meng, Tarel]. The proposed method is linear in N=nxm(size of image), the number of pixels in the image. Restoring the dehazed image from the transmission map is O(N). All the methods are implemented in MATLAB 2018a, and we evaluate them on the same machine. The average run time using two image resolutions shown in Table IV. In [24], it has been shown that state-of-the-art methods are taking a few seconds in an environment on the same machine (Intel CPU 3.40 GHz and 16GB memory and NVIDIA GeForce GTX 285 (1 GB) graphics card). Our method works very well compared to other state-of-the-works.

Table IV Run Time

Image Size	Ours	He[6]	Fattal[5]	Meng[30]	Tarel[7]
427x370/ 640x480	3.028 sec/ 8.637	35 mints (Average)	10 mints (Average)	12 mints (Average)	2 mints (Average)

4. Discussion, shortcoming, and future scope

This paper addresses the classical constrained ill-posed inverse single image Dehazing problem, broadly visibility improvement that scales down single image visual quality and visibility which has immense applications. The efficient DnCNN model is a popular blind denoising feed-forward very deep learning architecture. The depth of the image is recovered through DnCNN blind denoising, cleaning hidden layers of transmission map without losing original image information. The added effect of DnCNN denoising is to remove blurring, blocking, and resolution problems. Atmospheric light is estimated through an average of 1% maximum intensity pixels of each channel. Adaptable haziness factor makes the algorithm effective and rich [32]. Our algorithm is linear. State-of-the-art dehazing techniques recover the haze-free image with either compromise of time and memory complexity or visual quality [4-7, 29]. Our approach is fast, has low computational complexity, and efficient with null hallow effect, no colour shifting, and improved visibility. Finally, this method is adaptable to a wide range of degraded images on the day, night, rainy, underwater conditions with natural and synthetic image datasets and compared to seven benchmark algorithms with GT O-Haze dataset and statistical parameters like PSNR, SSIM, Entropy, and compression ratio.

References

[1] Sung Cheol Park, Min Kyu Park, and Moon Gi Kang ,Super-Resolution Image Reconstruction: A Technical Overview, IEEE Signal Processing Magazine, May 2003. 1053-5888/03/$17.00©2003IEEE .

[2] Yoav Y. Schechner, Member, IEEE, and Yuval Averbuch, Regularized Image Recovery in Scattering Media , IEEE Transactions on Pattern Analysis and Machine Intelligence, Vol. 29, No. 9, September 2007 .

[3] W. Wang, X. Yuan, Recent Advances in Image Dehazing, IEEE Journal of Automatica Sinica, Vol. 4, No. 3, July 2017

[4] R Tan, Visibility in Bad Weather from A Single Image, 2008 CPVR, IEEE Explore, DOI: 10.1109/CVPR.2008.4587643,ISSN:1063-6919.

[5] R Fattal, Single Image Dehazing, ACM Transaction on Graphics(TOG), vol-27, Issue-3,August2008.

[6] K.,He, J., Sun, and X., Tang,: Single image haze removal using dark channel prior", IEEE Conference on Computer Vision and Pattern Recognition, Miami, FL, 2009,pp- 1956 – 1963

[7] J. P. Tarel , Hautiere, N., Fast visibility restoration from a single color or gray level image, IEEE 12th International conference on Computer Vision (2009) 2201 – 2208.

[8] D Berman, T Treibitz, S Avidan, Non-local Image Dehazing, CVPR2016.

[9] J. P. Oakley and B. L. Satherley, "Improving image quality in poor visibility conditions using a physical model for contrast degradation," IEEE Trans. Image Process., vol. 7, no. 2, pp. 167°179, Feb. 1998.

[10] H. Koschmieder, Theorie der horizontalen sichtweite, Beitr.Phys. Freien Atm., vol. 12, 1924, pp. 171–181.

[11] E J McCartney , Optics of the Atmosphere: Scattering by Molecules and Particles, New York, NY, USA:Wiley, 1976.

[12] D Das, S Roy, S S Chaudhuri, Dehazing Technique based on Dark Channel Prior model with Sky Masking and its quantitative analysis, CIEC16, IEEE Explore, IEEE Conference ID: 36757 .

[13] S Roy, S S Chaudhuri, Modelling and control of sky pixels in visibility improvement through CSA , IC2C2SE2016

[14] S Roy, S S Chaudhuri, Modeling of Ill-Posed Inverse Problem, IJMECS, 2016, 12,pp-46-55

[15] S Roy, S S Chaudhuri, Low Complexity Single Colour Image Dehazing Technique,Intelligent Multidimensional Data and Image Processing, June 2018, IGI Global.

[16] Image Denoising Using Wavelets ,— Wavelets & Time Frequency — ,Raghuram Rangarajan Ramji Venkataramanan Siddharth Shah ,December 16, 2002 .

[17] Siraj Sidhik , Comparative study of Birge–Massart strategy and unimodal thresholding for image compression using wavelet transform ,OPTIK, ELSEVIER, 2015,Optik 126 (2015) 5952–5955 .

[18] Wavelet Signal and Image Denoising, E. Hostalkova ´, A. Prochazka ,Institute of Chemical Technology Department of Computing and Control Engineering.

[19] Comparative Analysis of Filters and Wavelet Based Thresholding Methods for Image Denoising, Anutam, Rajni, SBSSTC, SBSSTC, Ferozepur, Punjab.

[20] Discrete Wavelet Transform Decomposition Level Determination Exploiting Sparseness Measurement, Lei Lei, Chao Wang, X Liu, World Academy of Science, Engineering and Technology International Journal of Electrical and Computer Engineering Vol:7, No:9, 2013.

[21] D. L. Donoho and I. M. Johnstone, ―Adatpting to unknow smoothness via wavelet shrinkage,‖ Journal of the American Statistical Association, vol. 90, no. 432, pp. 1200-1224, December 1995. doi:10.1.1.161.8697.

[22] A Dixit, P Sharma, A Comparative Study of Wavelet Thresholding for Image Denoising, I.J. Image, Graphics and Signal Processing, 2014, 12, 39-46 , DOI: 10.5815/ijigsp.2014.12.06

[23] H Guo, C S Burrus, Fast Approximate Fourier transform via Wavelets Transform , Proceedings of the SPIE, Volume 2825, p. 250-259 (1996).

[24] W Ren, S Liu, H Zhang, J Pan, X Cao, M-H Yang, Single image dehazing via multi-scale convolutional neural Networks ,European conference on computer vision,Springer, Cham,October2016, pp.154-169.

[25] L. Kratz and K. Nishino, "Factorizing scene albedo and depth from a single foggy image," in Proc. IEEE 12th Int. Conf. Comput. Vis. (ICCV), Sep./Oct. 2009, pp. 1701–1708.

[26] Gaofeng MENG, Ying WANG, Jiangyong DUAN, Shiming XIANG, Chunhong PAN , Efficient Image Dehazing with Boundary Constraint and Contextual Regularization , IEEE International Conference on Computer Vision , 2013 IEEE, pp.617-624.

[27] Q Zhu, J Mai, L Shao , A Fast Single Image Haze Removal Algorithm Using Color Attenuation Prior , IEEE Transactions on Image Processing, Vol. 24, No. 11, November 2015, pp.3522-3533

[28] Dana Berman, Tali Treibitz, Shai Avidan, Non-Local Image Dehazing, IEEE, (CVPR2016), pp.1674-1682.

[29] J Kopf, B Neubert, B Chen, M Cohen, D Cohen-0r, O Deussen, M Uyttendaele, D Lischinski, Deep photo: Model- based photograph enhancement and viewing, ACM transactions on graphics (TOG),2008

[30] K Zhang, WZuo, Y Chen, D Meng, L Zhang , Beyond a Gaussian Denoiser: Residual Learning of Deep CNN for Image Denoising ,IEEE TIP2017

[31] Y Chen, T Pock, Trainable Nonlinear Reaction Diffusion:A Flexible Framework for Fast and Effective Image Restoration, IEEE ,TPAM, vol(20),I(20),2016

[32] S Roy, S S Chaudhuri, Fast Single Image Haze Removal Scheme Using Self-Adjusting: Haziness Factor Evaluation, IGI Global, Jan 2019.

[33] E. B. Goldstein. Sensation and perception. 1980.

[34] A. J.Preetham,P.Shirley,and B.Smits. A practical analytic model for daylight, SIGGRAPH, pages 91–100, 1999.

[35] Kim, J.-H., Jang, W.-D., Sim, J.-Y., and Kim, C.-S. (2013). Optimized contrast enhancement for real-time image and video dehazing. Journal of Visual Communication and Image Representation, 24(3):410–425.

[36] L. Kubecka, J. Jan, and R. Kolar, “Retrospective illumination correction of retinal images,” Journal of Biomedical Imaging, vol. 2010, p. 11, 2010.

[37] T Knoll, J Knoll, PSAC, Abode Photoshop 1990.

[38] K Tang, J Yang, J Wang, Investigating Haze-Relevant Features in a Learning Framework for Image Dehazing, IEEE Conference on Computer Vision and Pattern Recognition, 2014.

[39] D Xu, C Xiao, J Yu, Color Preserving Defog method for foggy and Haze Scenes, VISAPP 2009. [40] C Xiao, J Gan, Fast Dehazing using Guided Joint Bilateral Filter, Springer Verlag 2012.

[41] P Mahamadi, A E Moghadam, S Shirani, Subjective and Objective Quality Assessment of Image: A Survey, Mejlesi Journal of Electrical Engineering, vol-9(1),2015.

[42] C O Ancuti, R Timofti, C D Vleeschouwer, O-Haze:A Dehazing BenchMark with Real Hazy and Haze-free Outdoor Images,CVPRW 2018.

[43] S Roy, S S Chaudhuri, WLMS-based Transmission Refined Self-Adjusted No Reference Weather Independent Image Visibility Improvement, IETE Journal of Research, September, 2019.